Supplement of Hydrol. Earth Syst. Sci., 29, 1759–1782, 2025
https://doi.org/10.5194/hess-29-1759-2025-supplement

Hydrology and Earth System Sciences
Open Access
EGU

Supplement of

From hydraulic root architecture models to efficient macroscopic sink terms including perirhizal resistance: quantifying accuracy and computational speed

Daniel Leitner et al.

Correspondence to: Daniel Leitner (d.leitner@fz-juelich.de)

S1 Derivation of the expression of water flux at root-soil interface

In this section, we derive Eqn (22), the volumetric flow rate q_{sr} towards the soil-root interface through the perirhizal zone, as a function of the average (bulk) soil matric potential in the perirhizal zone and the soil matric potential at the soil-root interface.

We start with Eqn (4) from Schröder et al. (2008), the steady-rate analytical solution for the matric flux potential around a single root:

$$\Phi(a) = \Phi_{prhiz} + (J_{sr} r_{sr} - J_{prhiz} r_{prhiz}) \left[\frac{a^2/a_{root}^2}{2(1-\rho^2)} + \frac{\rho^2}{1-\rho^2} \left(\ln \frac{a_{prhiz}}{r} - 0.5 \right) \right] + J_{prhiz} r_{prhiz} \ln \frac{a}{a_{prhiz}}, \tag{1}$$

where a is the radial distance from the root surface, $\Phi(h_c) = \int_{-\infty}^{h_c} K(h)dh$ is the matric flux potential, J is the Darcy flux of water (and $q = 2a\pi l_{root} J$ is the volumetric flow rate), $\rho = \frac{a_{prhiz}}{a_{rs}}$ and the subscripts $_{rs}$ and $_{prhiz}$ indicate radial positions at the soil-root interface and the outer end of the perirhizal zone, respectively.

Our aim is to express the water flux at the soil-root interface as a function of the average (bulk) soil matric potential, h_s, and the soil matric potential at the soil-root interface, h_{sr}. We define $\bar{a} \approx \alpha a_{prhiz}$ as the radial distance from the root at which the water content, θ, is equal to the mean perirhizal water content, i.e., $\theta(\bar{a}) = \bar{\theta}$. According to De Jong Van Lier et al. (2008), $\alpha \approx 0.53$. In the following, we will make the assumption of a no-flux outer boundary condition, $J_{prhiz} = 0$, i.e., competition between neighbouring roots. At $a = a_{root}$, Eqn (1) becomes:

$$\Phi_{sr} = \Phi(a_{root}) = \Phi_{prhiz} + (J_{sr} a_{root}) \left[\frac{1}{2(1-\rho^2)} + \frac{\rho^2}{1-\rho^2} (\ln \rho - 0.5) \right], \tag{2}$$

and with $a = \bar{a} \approx \alpha a_{prhiz}$, Eqn (1) becomes

$$\bar{\Phi} = \Phi(\bar{a}) = \Phi_{prhiz} + J_{sr} a_{root} \left[\frac{\alpha^2 \rho^2}{2(1-\rho^2)} + \frac{\rho^2}{1-\rho^2} (\ln(-\alpha) - 0.5) \right]. \tag{3}$$

We now replace the unknown soil matric potential at the outer boundary of the perirhizal zone, h_{prhiz}, with the average value in the perirhizal zone, h_s, which we can approximate in the coupled model at each time step with the value of the corresponding macroscopic soil element. This means that all rhizosphere models within the same soil control element have the same h_s value. From Eqn (3) we can express Φ_{prhiz} as a function of $\bar{\Phi}$:

$$\Phi_{prhiz} = \bar{\Phi} - J_{sr} r_{sr} \left[\frac{\alpha^2 \rho^2}{2(1-\rho^2)} + \frac{\rho^2}{1-\rho^2} (\ln(-\alpha) - 0.5) \right], \tag{4}$$

and insert into Eqn 2 to get

$$\bar{\Phi} - \Phi_{sr} = (J_{sr} a_{root}) \left[\frac{1 + 2\rho^2 (\ln \rho - 0.5) - \alpha^2 \rho^2 + 2\rho^2 (\ln \alpha + 0.5)}{2(\rho^2 - 1)} \right]. \tag{5}$$

Using the definition of $K_{prhiz} = \frac{\Phi(h_s) - \Phi(h_{sr})}{h_s - h_{sr}}$ and rearranging gives:

$$\frac{\bar{\Phi} - \Phi_{sr}}{h_s - h_{sr}} \frac{\bar{h} - h_{sr}}{a_{root}} = J_{sr} \left[\frac{1 + 2\rho^2 (\ln \rho - 0.5) - \alpha^2 \rho^2 + 2\rho^2 (\ln \alpha + 0.5)}{2(\rho^2 - 1)} \right] \tag{6}$$

and

$$J_{sr} = \frac{K_{prhiz}}{a_{root}} B (h_s - h_{sr}), \tag{7}$$

$$q_{sr} = 2\pi l_{root} K_{prhiz} B (h_s - h_{sr}), \tag{8}$$

where $B = \frac{2(\rho^2 - 1)}{1 - \alpha^2 \rho^2 + 2\rho^2 (\ln \rho + \ln \alpha)}$. Note that soil matric potential difference $h_s - h_{sr} = H_s - H_{sr}$.

S2 Supplementary figures

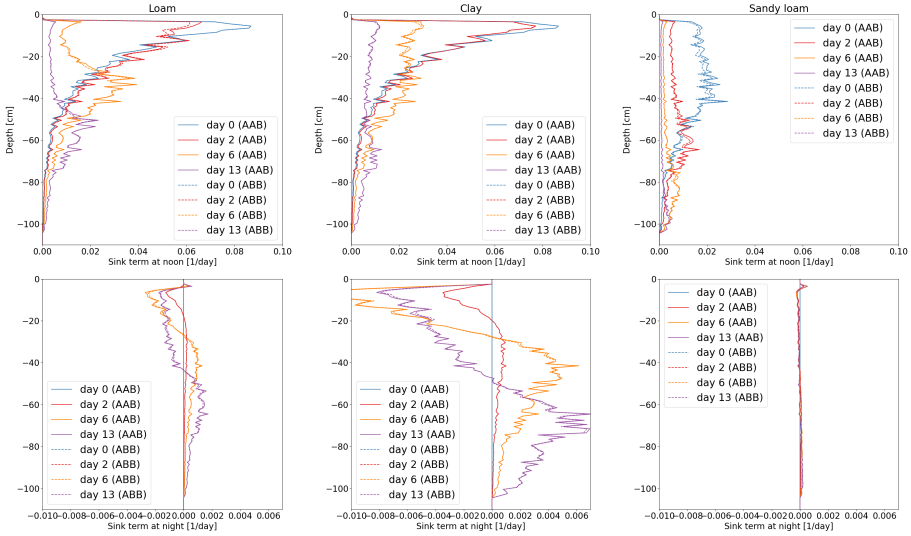

Figure S1. Vertical RWU of spring barley using the full hydraulic 3D model during noon (top row) and redistribution during night (bottom row) of spring barley for loam (left column), clay (mid column), and sandy loam (right column) in a 1D soil grid. Solid lines represent the results using Voronoi method (AAB), while dashed lines use RLD based outer radii (ABB).

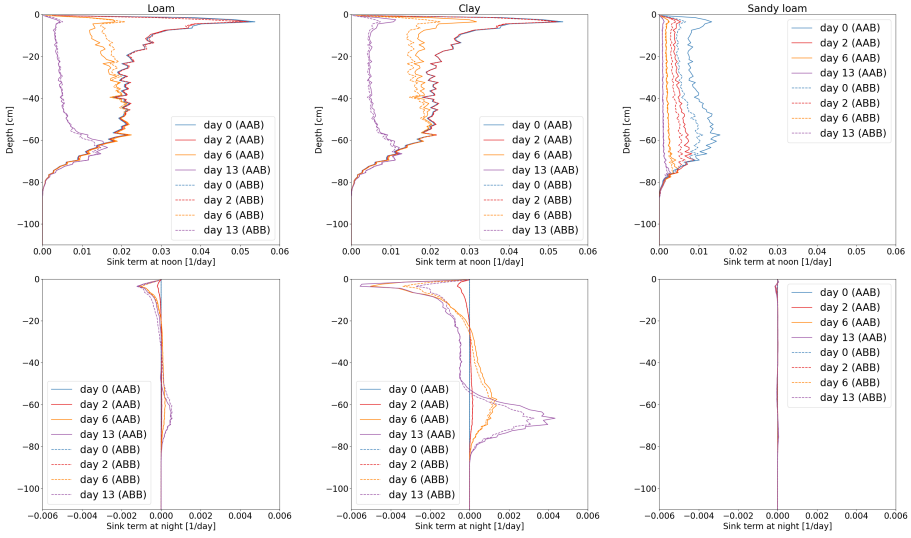

Figure S2. Vertical RWU of the full hydraulic 3D model during noon (top row) and redistribution during night (bottom row) of maize for loam (left column), clay (mid column), and sandy loam (right column) in a 1D soil grid. Solid lines represent the results using Voronoi method (AAB), while dashed lines use RLD based outer radii (ABB).

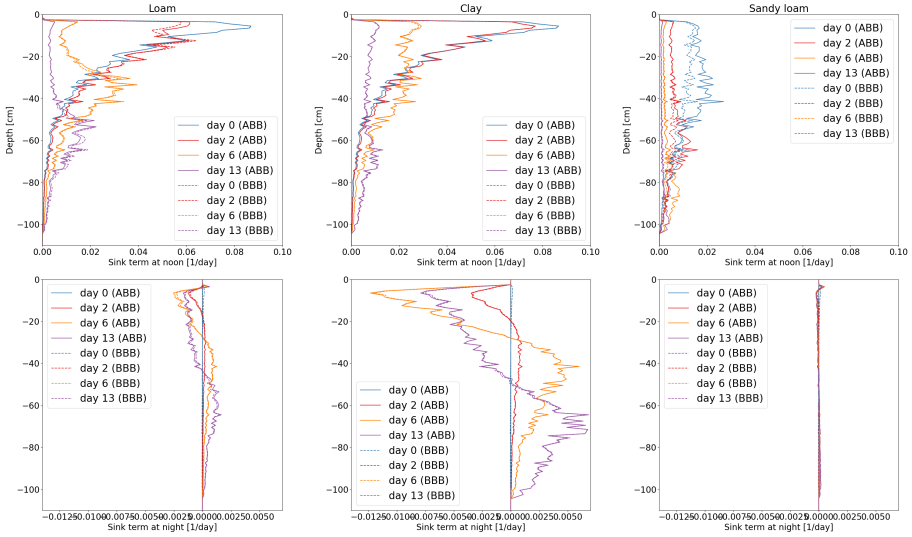

Figure S3. Comparison of the full hydraulic model (ABB) with the aggregated model (BBB) for spring barley using a 1D soil grid. Vertical RWU during noon (top row) and redistribution during night (bottom row) of spring barley for loam (left column), clay (mid column), and sandy loam (right column).

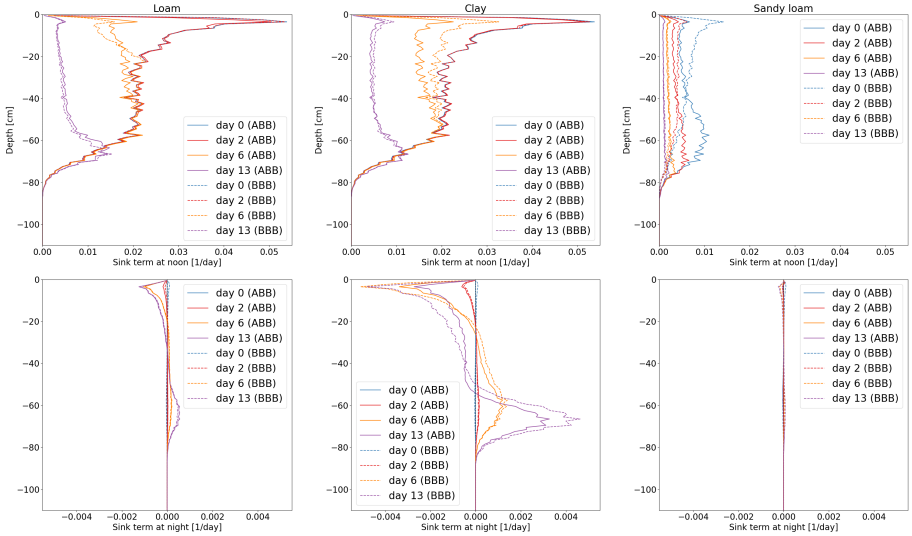

Figure S4. Comparison of the full hydraulic model (ABB) with the aggregated model (BBB) for maize using a 1D soil grid. Vertical RWU during noon (top row) and redistribution during night (bottom row) of maize for loam (left column), clay (mid column), and sandy loam (right column).

References

35 De Jong Van Lier, Q., Van Dam, J., Metselaar, K., De Jong, R., and Duijnisveld, W.: Macroscopic root water uptake distribution using a matric flux potential approach, Vadose Zone Journal, 7, 1065–1078, 2008.

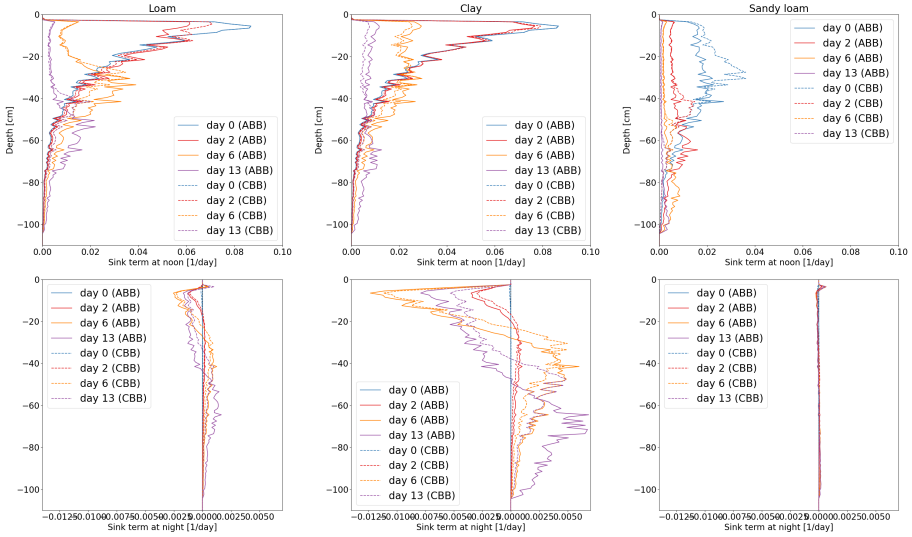

Figure S5. Comparison of the full hydraulic model (ABB) and the parallel root model (CBB) for spring barley using a 1D soil grid. Vertical RWU during noon (top row) and redistribution during night (bottom row) of spring barley for loam (left column), clay (mid column), and sandy loam (right column).

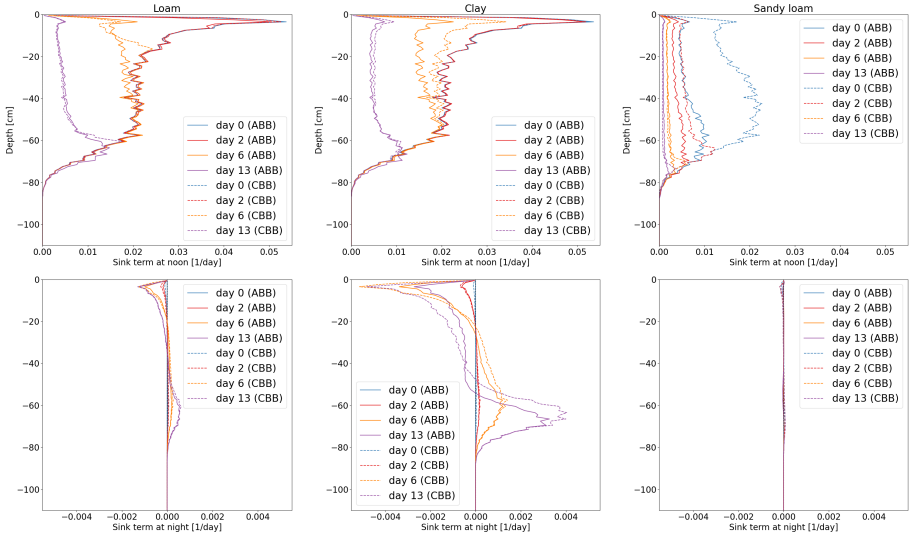

Figure S6. Comparison of the full hydraulic model (ABB) and the parallel root model (CBB) for maize using a 1D soil grid. Vertical RWU during noon (top row) and redistribution during night (bottom row) of maize for loam (left column), clay (mid column), and sandy loam (right column).

Schröder, T., Javaux, M., Vanderborght, J., Körfgen, B., and Vereecken, H.: Effect of local soil hydraulic conductivity drop using a three-dimensional root water uptake model, Vadose Zone Journal, 7, 2008.